Atherosclerosis 346 (2022) 86–97

Contents lists available at ScienceDirect

Atherosclerosis

journal homepage: www.elsevier.com/locate/atherosclerosis

PCSK9 promotes arterial medial calcification

Maria Giovanna Lupo [a], Alessandro Bressan [a], Maristella Donato [b], Paola Canzano [c], Marina Camera [c,d], Paolo Poggio [c], Maria Francesca Greco [e], Mariangela Garofalo [b], Sara De Martin [b], Giovanni Panighel [b], Massimiliano Ruscica [e], Andrea Baragetti [e], Valentina Bollati [f,g], Elisabetta Faggin [a], Marcello Rattazzi [a,h], Alberico L. Catapano [e,i,**], Nicola Ferri [a,*]

[a] Dipartimento di Medicina, Università degli Studi di Padova, Padua, Italy
[b] Dipartimento di Scienze del Farmaco, Università degli Studi di Padova, Padua, Italy
[c] Centro Cardiologico Monzino IRCCS, Milan, Italy
[d] Dipartimento di Scienze Farmaceutiche, Università degli Studi di Milano, Milan, Italy
[e] Dipartimento di Scienze Farmacologiche e Biomolecolari, Università degli Studi di Milano, Milan, Italy
[f] EPIGET Department of Clinical Sciences and Co mMunity Health, Università degli Studi di Milano, Milan, Italy
[g] Dipartimento di Scienze Cliniche e di Comunità, Università degli Studi di Milano, Milan, Italy
[h] Medicina Interna I^, Cà Foncello Hospital, Treviso, Italy
[i] IRCCS Multimedica Hospital, Milan, Italy

ARTICLE INFO

Keywords:
PCSK9
Calcification
Smooth muscle cells
Vescicles
Chronic kidney disease

ABSTRACT

Background and aims: A complex interplay among chronic kidney disease (CKD), lipid metabolism and aortic calcification has been recognized. Here we investigated the influence of kidney function on PCSK9 levels and its potential direct action on smooth muscle cells (SMCs) calcification.

Methods and Results: In a cohort of 594 subjects, a negative association between glomerular filtration rate and plasma PCSK9 was found. Atherosclerotic cardiovascular disease, as co-morbidity, further increased PCSK9 plasma levels. Diet-induced uremic condition in rats led to aortic calcification and increased total cholesterol and Pcsk9 levels in plasma, livers, and kidneys. Both human and rat SMCs overexpressing human PCSK9 ($SMCs^{PCSK9}$), cultured in a pro-calcific environment (2.0 mM or 2.4 mM inorganic phosphate, P_i) showed a significantly higher extracellular calcium (Ca^{2+}) deposition compared to control SMCs. The addition of recombinant human PCSK9 did not increase the extracellular calcification of SMCs, suggesting the involvement of intracellular PCSK9. Accordingly, the further challenge with evolocumab did not affect calcium deposition in $hSMCs^{PCSK9}$. Under pro-calcific conditions, $SMCs^{PCSK9}$ released a higher number of extracellular vesicles (EVs) positive for three tetraspanin molecules, such as CD63, CD9, and CD81. EVs derived from $SMCs^{PCSK9}$ tended to be more enriched in calcium and alkaline phosphatase (ALP), compared to EVs from control SMCs. In addition, PCSK9 has been detected in $SMCs^{PCSK9}$-derived EVs. Finally, $SMCs^{PCSK9}$ showed an increase in pro-calcific markers, namely bone morphogenetic protein 2 and ALP, and a decrease in anti-calcific mediator matrix GLA protein and osteopontin.

Conclusions: Our study reveals a direct role of PCSK9 on vascular calcification induced by higher inorganic phosphate levels associated with renal impairment. This effect appears to be mediated by a switch towards a pro-calcific phenotype of SMCs associated with the release of EVs containing Ca^{2+} and ALP.

1. Introduction

Cardiovascular disease (CVD) is the leading cause of morbidity and mortality among patients with chronic kidney disease (CKD) [1]. Even after adjustment for known CV risk factors, including diabetes and hypertension, mortality risk progressively increases as CKD worsens [2,3].

* Corresponding author. Università degli Studi di Padova, Dipartimento di Medicina, Via Giustiniani 2, 35128, Padua, Italy.
** Corresponding author. Università degli Studi di Milano, Dipartimento di Scienze Farmacologiche e Biomolecolari , I.R.C.C.S. MultiMedica, Milan, Via Balzaretti 9, 20133, Milan, Italy.
E-mail addresses: alberico.catapano@unimi.it (A.L. Catapano), nicola.ferri@unipd.it (N. Ferri).

https://doi.org/10.1016/j.atherosclerosis.2022.01.015
Received 12 July 2021; Received in revised form 14 January 2022; Accepted 19 January 2022
Available online 22 January 2022

Cardiovascular abnormalities in CKD are associated with traditional (*e.g.*, diabetes and hypertension) and nontraditional CKD-related CVD risk factors (*e.g.*, mineral and bone disease abnormalities, anemia, inflammation, and oxidative stress), as well as dialysis-related factors [4]. As glomerular filtration rate (GFR) declines, the vascular calcification increases, an event that is associated with higher mortality in end-stage kidney disease (ESKD).

Calcification of the *subintima* and *media* of large vessels is a result of the progressive reduction in the renal excretion of calcium (Ca^{2+}) and phosphate (Pi), leading to a dramatic increase in their plasma concentrations [5]. In addition, during the course of CKD, significant changes in lipoproteins profile have been documented with an increase in triglycerides (TG) and very low-density lipoprotein-cholesterol (VLDL-C) levels, a reduction in high-density lipoprotein-cholesterol (HDL-C) and minimal changes in low-density lipoprotein-cholesterol (LDL-C) [6,7]. However, qualitative modifications of LDL occur, resulting in an accumulation of small-dense LDL [8]. Similarly, lipoprotein(a) [Lp(a)] is increased [9], and considered as an independent risk factor for CVD in hemodialysis patients [10].

Any dyslipidemia associated with a particular pathological condition deserves the assessment of the plasma levels of one of the major circulating players of lipid and cholesterol homeostasis, *i.e.*, proprotein convertase subtilisin/kexin type 9 (PCSK9). PCSK9 emerged in the last decade as a valuable pharmacological target in the prevention of the most severe forms of atherosclerotic cardiovascular disease [11], including those associated with CKD [12]. Beyond the effect on plasma cholesterol, PCSK9 showed wide range of effects on patho-physiological mechanisms associated with cellular cholesterol handling, including the accumulation of visceral adipose tissue [13], and the release of insulin by pancreas [14]. PCSK9 plasma levels do not seem to correlate with GFR in studies recruiting a small number of patients [15,16], while a "suggestive" positive association was recently observed in the large cohort of IMPROVE European study [17]. However, the strongest elevation of plasma PCSK9 is observed in protein wasting conditions (such as nephrotic syndrome or peritoneal dialysis) [18], where alterations in lipid metabolism and exacerbation of vascular atherosclerotic calcifications occur [19]. Nonetheless, a role for PCSK9 in vascular and aortic valve calcification (AVC) is emerging both in clinical and experimental settings. PCSK9 levels correlate with higher risk of coronary artery calcification (CAC) in patients with familial hypercholesterolemia (FH) under statin treatment [20]. In patients with and without AVC, plasma PCSK9 levels correlate with the presence of calcific aortic valve disease (CAVS) but not with its severity [21]. A retrospective analysis of 103,083 individuals revealed that subjects carrying the *loss-of-function* (LOF) R46L variant in PCSK9 are characterized by lower levels of LDL-C, Lp(a) and a lower risk of CAVS [22], results that were more recently confirmed by a pooled data analysis [23]. Thus, genetic analyses predict that an intervention aimed at reducing PCSK9 could prevent CAVS. Although clinical evidence on this effect is still lacking, a recent subgroup analysis of the FOURIER trial revealed that the monoclonal antibody anti PCSK9, evolocumab, could decrease CAVS incidence in patients with CVD [24]. Moreover, results of an unpaired cross-sectional study indicated that statins and/or PCSK9 inhibitors promote vascular calcification, while the evaluation of a longitudinal analysis suggests that CAC might be prevented with add-on PCSK9 inhibitors to statin [25]. Finally, coronary intravascular ultrasound imaging of statin-treated patients showed that the addition of evolocumab for 76 weeks did not produce significant changes in plaque composition compared with statin monotherapy, including vascular calcium content [26], thus suggesting a lack of therapeutic efficacy of anti PCSK9 monoclonal antibodies on vascular calcification.

Experimentally, overexpression of a *gain-of-function* (GOF) D377Y variant of PCSK9, strongly promoted aortic calcification, an effect partially dependent on sortilin expression [27] - an important regulator of lipoprotein metabolism [28] and vascular calcification [29] - that directly binds to PCSK9 [30]. Finally, we have previously observed that *Pcsk9* null mice have lower total calcium content in aortic valve leaflets and in valve interstitial cells compared to wild-type mice [31].

The mechanisms promoting the initiation and progression of vascular calcification show similarities to those of physiological bone formation, including osteo/chondrogenic transdifferentiation, decreased availability of calcification inhibitors, extracellular vesicle (EVs) release [32], and remodeling of extracellular matrix [33]. Vascular smooth muscle cells (SMCs) play a key role during vascular calcification [34]. Interestingly, PCSK9 has been detected in human atherosclerotic plaques [35], and around calcification areas formed by synthetic SMCs in patients with acute aortic dissection (AAD) [36]. These observations brought us to further investigate a potential direct role of PCSK9 in vascular calcification associated with renal impairment.

2. Materials and methods

2.1. Study population

Subjects were enrolled in the "Progressione delle Lesioni Intimali Carotidee (PLIC) Study", a general population-based study [37]. The study was approved by the Scientific Committee of the University of Milan (SEFAP/Pr.0003). An informed consent was obtained by subjects (all over 18 years of age), in accordance with the Declaration of Helsinki. Subjects were included in the study following these criteria: inflammatory or infectious disorders, congenital or hereditary kidney diseases, previous or current dialysis (either peritoneal or hemodialysis), glomerulonephritis, cardiovascular events in the previous six months, previous major cardiac or vascular surgery, microvascular complications (either as retinopathy, neuropathy, foot ulcers or gangrenes), malignant neoplasms, and thyroid dysfunction were excluded from the study. Systolic and diastolic blood pressure, Body Mass Index (BMI), and waist and waist/hip ratio were measured. Information on presence of hepatic steatosis, available on a subgroup of 133 subjects, was defined via ultrasound, according to already published protocols [37]. Total body fat mass and abdominal fat mass were measured using Dual-X Ray Absorbimetry, as previously published [37]. Blood samples were collected from the antecubital vein after 12 h fasting on NaEDTA tubes (BD Vacuette®, Franklin Lakes, NJ, USA) and then, centrifuged at 3.000 rpm for 12 min (Eppendorf 580r, Eppendorf, Hamburg, Germany) for biochemical parameters profiling including: total cholesterol, HDL-C, triglycerides, apolipoprotein B (ApoB), ApoA-I, glucose, liver enzymes, creatinine and creatinine-phospho kinase (CPK). Measurements were performed using immuno-turbidimetric and enzymatic methods thorough automatic analyzers (Randox, Crumlin, UK). LDL-C was derived from the Friedewald formula. Renal function was defined by GFR according to the Cockroft-Gault formula. Atherosclerotic calcifications were defined by ultrasound-based analysis of bilateral carotid arteries as previously described, as the presence of intima-media thickness (IMT) above the 75th percentile of the median IMT for a Caucasian population according to the American Society of Echocardiography (ASE) guidelines. Subclinical atherosclerosis (SCA) was defined when mean IMT was $\geq$1.3 mM or in presence of focal atherosclerotic lesions larger than 1.3 mM using a manual caliper in longitudinal view either in far or near wall and over every carotid tract (common, bulb section, bifurcation, internal or external branches). Ultrasonic scanning of the lesions was performed in longitudinal, transverse, and oblique sections. Echolucency of the atherosclerotic calcifications was defined by an independent ultrasound-based system (HM70a Plus, Samsung Ultrasound System®) equipped with an automated software to differentiate Hypo-, Mild- and Hyper-echogenic atherosclerotic calcifications according to grayscale. Also, common carotid (CIMT) was measured (1 cm from the bulb) in longitudinal view, far wall, by high resolution B-mode ultrasound-based system (Vivid S5, GE Healthcare®, Wauwatosa, WI, USA) connected to a linear probe (4.0 × 13.0 MHz frequency; 14 × 48 mM footprint, 38 mM field of view). In two scans performed by the same operator in 75 subjects, the mean difference in IMT was 0.005 ± 0.002 mM and the

coefficient of variation (CV) was 1.93%. The correlation between two scans was significant ($r = 0.96$; $p < 0.0001$).

Ankle-Brachial Index (ABI) was measured using an automatic blood pressure/Doppler monitor (Omron® model HEM-705 CP, Japan). The systolic pressure at the brachial artery was measured three times with the subject in a supine position, at 2-min intervals. Next, systolic blood pressure at the posterior tibial artery was measured three times in both legs at 2-min intervals. A ratio of the two term (respectively) was then calculated. Peripheral artery disease was defined in presence of ABI<0.9.

2.1.1. PCSK9 plasma quantification

Plasma PCSK9 concentrations were measured with a commercial ELISA kit (R&D System) able to recognize free and LDLR-bound PCSK9. Plasma samples were diluted 1:20, according to manufacturer's instructions, and incubated onto a microplate precoated with a monoclonal antibody specific for human PCSK9. Sample concentrations were obtained by generating a four-parametric logistic (4 PL) curve-fit using GraphPad Prism v8.2.1® for Windows. The minimum detectable concentration was 0.219 ng/mL. Intra- and inter-assay CV were 5.4 ± 1.2% and 4.8 ± 1.0%, respectively [17].

2.1.2. Statistical analysis

Statistical analyses were performed using SPSS® v.23.0 for Windows® (IBM Corporation®) software. Shapiro–Wilk test was performed to verify the normal or non-normal distribution of continuous variables. In Supplemental Table 1 we compared raw clinical data by univariate analyses (ANOVA for linear values, chi-square test for dichotomous variables). Inter-variable co-linearity was tested to derive the Variation Inflation Factor (VIF) to exclude redundant covariates. Box plots for data distributions, reporting mean values with 10th to 90th upper and lower bounds, were generated using GraphPad Prism 5® for Windows®. For all analyses, p-values < 0.05 were considered statistically significant.

2.2. In vivo experiments

2.2.1. Animal model

Twenty-two 10-week old male rats (Sprague-Dawley strain) were purchased from Charles River Laboratories ITALIA S.r.L. and housed in the facility at the Department of Pharmaceutical and Pharmacological Sciences, University of Padua, Padua, Italy. They were kept in pathogen-free and temperature-controlled rooms (25 °C), following the circadian rhythm of 12 h of light and 12 h of dark.

Rats were fed a standard diet (SD) for seven days, after which they were randomized in control group (n = 11) or uremic group (n = 11), following a well-established uremic rat model [38] according to which an adenine-rich diet causes renal damage and thus severe renal impairment [39,40]. Food intake, as well as animal weights, were weekly monitored during all the period of treatment. Control diet contained 19% of proteins, 20% lactose, 1.2% phosphate, and 1% calcium, while uremic diet 4.5% proteins, 20% lactose, 1.2% phosphate, 0.5% adenine, and 1% calcium. Both were purchased from Mucedola S.r.L., Italy.

Urines were collected every two weeks by means of metabolic cages and after 6 weeks of treatment rats were sacrificed and livers, aortas, kidneys, and blood collected. Euthanasia was performed by deep anesthesia with 1.5%–4.5% isoflurane and perfusion with physiological solution. Both during the experimentation period and the sacrifice, the rats were continuously subjected to medical controls to check their health status, according to the Italian Guidelines for the animal experimentation. The investigation conforms to the European Commission Directive 2010/63/EU and was performed after the approval of the Italian Ministry of Health (Auth. no. 278/2017-PR).

GPower software [41] has been utilized to calculate the appropriate number of animals to perform an accurate statistical analysis. Parameters set: α-error 5%, power 80%, effect-size 0.35%. The primary endpoint was the determination of aortic calcium in the aortas.

Sera were separated by centrifugation at 5,000*g* and stored at −80 °C until further analyses. The thoracic aorta was freeze-dried for calcium quantification. A distal portion (0.3 cm) was included in OCT compound tissue tek (Akura) for histological analysis. The abdominal aortas, as well as the livers and the kidneys, were snap frozen and stored at −80 °C until further analyses.

2.2.2. Evaluation of arterial medial calcification

The examination of arterial medial calcification was performed on transverse cryosections that were processed for von Kossa staining using the standard method. To quantitatively evaluate the degree of aortic medial calcification, freeze-dried aortic tissues were weighed and hydrolyzed overnight in 1 mL of HCl 0.6 N at room temperature. The Ca^{2+} content of the supernatant was determined using commercially available Calcium kits (Chema Diagnostica) and normalized to wet tissue weight (mg Ca^{2+}/mg wet weight).

2.2.3. Immunohistochemistry

Pcsk9 expression in aortic rat tissues was analyzed by immunohistochemistry using the EXPOSE Mouse and Rabbit Specific HRP/DAB Detection IHC Kit (Abcam) according to the manufacturer's protocol. Briefly, transverse cryosections (8 μm) adjacent to those processed with the von Kossa were stained with polyclonal PCSK9 antibody (Abcam). The blocking of endogenous peroxidase was performed by incubation of sections in a hydrogen peroxidase solution. Controls for the indirect-immunohistochemistry experiments were as follows: 1) non-immune immunoglobulin G (IgG) instead of primary antibody and 2) the second antibody alone. The image acquisition was performed using a Leica microscope assembled with a DFC 420 camera.

2.2.4. Pcsk9 plasma quantification

Plasma Pcsk9 was measured with the commercial ELISA kit specific for rat Pcsk9 (Elabscience), according to manufacturer's instructions. Sample concentrations were obtained by generating a 4 PL curve-fit with GraphPad Prism v8.2.1. The minimal detectable concentration was 0.47 ng/mL, with CV less than 10%.

2.2.5. Western blotting

Kidneys and livers (100 mg) were homogenized in 1 mL of lysis buffer containing 1% NP-40, 150 mM NaCl and 50 mM Tris-HCl at pH 7.5. Protein concentration was assessed by bicinchoninic acid (BCA) assays (EuroClone), accordingly to manufacturer's instructions. 25 μg total protein extract/sample was separated on 4–20% SDS-Page gel (Bio-Rad) under denaturing and reducing conditions. Proteins were then transferred onto a nitrocellulose membrane using the Trans-Blot® Turbo™ Transfer System (Bio-Rad); 5% non-fat dried milk in tris-buffered saline containing 0.2% of tween 20 (TBST20) was used as blocking buffer. All the primary antibodies were diluted in 5% non-fat dried milk in TBST20 and incubated overnight at 4 °C in agitation; horseradish peroxidase (HPR)-conjugated secondary antibodies were diluted in blocking solution and membranes were left to incubate 2h at room temperature (RT) in agitation. Luminescence signals were acquired with c400 Azure Molecular Imager (Aurogene). Quantitative densitometric analysis was performed with ImageJ software. When used, stripping buffer was prepared according to Abcam's protocol. PCSK9 antibody was purchased from Abcam (cod. ab181142; dilution 1:1000), α-tubulin antibody from Sigma-Aldrich (cod. T6199; dilution 1:1000), secondary anti-mouse antibody was from Jackson ImmunoResearch (cod. 115-036-062; dilution 1:5000), and anti-rabbit antibody was from Jackson ImmunoResearch (cod. 113-036-045, dilution 1:5000).

2.2.6. Statistical analysis

Data are expressed as mean ± standard deviation. Differences between the two groups were analyzed via ANOVA test followed by

Bonferroni *post-hoc* correction or Student's *t*-test, when appropriate (GraphPad Prism v8.2.1® for Windows). *p*-values lower than 0.05 were considered statistically significant.

2.3. In vitro experiments

2.3.1. Cell cultures

Cell culture reagents were from EuroClone (Milan, Italy). Rat aortic smooth muscle cells (SMCs) were isolated by explant technique as previously described [42]. Human SMCs (A617 from human femoral artery) and rat SMCs were maintained in Dulbecco's Modified Eagle's Medium (DMEM) High Glucose supplemented by 10% Fetal Bovine Serum (FBS), 1% penicillin/streptomycin solution (10.000U/mL and 10 mg/mL, respectively), 1% L-glutamine 200 mM and 1% non-essential amino acids 100X solution. Simvastatin (Merck Sharp & Dohme Research Laboratories, Readington, NJ, USA) was dissolved in 0.1 M NaOH and the pH was adjusted to 7.4. This solution was then sterilized by filtration [43]. Evolocumab was kindly provided by Amgen S.r.L. and dissolved in cultured media at the final concentration of 10 μg/mL.

2.3.2. SMCs overexpressing human PCSK9

Human and rat vascular SMCs overexpressing human PCSK9 were generated by the means of HEK293-Phoenix (φNX-A) cells as previously described [44], using empty pBMN-IRES-puromycin vector or the same vector carrying human PCSK9 coding sequence under CMV promoter to generate, respectively, SMCs (control cells) and $SMCs^{PCSK9}$.

2.3.3. SMCs calcification

SMCs were seeded in 6-well trays at cellular density of 5×10^3 cells/well. After 24 h, media were replaced with complete fresh media supplemented with 2.5% of FBS or with calcific media (2.5% FBS + 2.0 mM or 2.4 mM inorganic phosphate (Pi) solution). Stock 100 mM Pi solution was composed by Na_2HPO_4 + NaH_2PO_4, pH 7.4. Treatments were refreshed every two days for a period of 6-days. The level of calcification was then measured by means of colorimetric assay (Chema Diagnostica) accordingly to manufacturer's instructions. Briefly, the cells were washed twice with PBS and incubated in agitation overnight at 4 °C in 500 μL of HCl 0.6 N. The day after the HCl supernatant were tested for Ca^{2+} presence basing on the reaction of *o*-cresolftalein complexone with calcium in an alkaline pH environment. Values were normalized for intracellular protein content, measured as described below.

2.3.4. Western blotting

SMCs were washed twice with PBS and homogenized in lysis buffer containing 1% NP-40, 150 mM NaCl and 50 mM Tris-HCl at pH 7.5. Protein concentration was assessed by BCA assays (EuroClone), accordingly to manufacturer's instructions. 25 μg total protein extract/sample were separated on 4–20% SDS-Page gel (Bio-Rad) under denaturing and reducing conditions. Proteins are then transferred onto a nitrocellulose membrane by using the Trans-Blot® Turbo™ Transfer System (Bio-Rad); 5% non-fat dried milk in tris-buffered saline containing 0.2% of tween 20 (TBST20) was used as blocking buffer. All the primary antibodies were diluted in 5% non-fat dried milk in TBST20 and incubate overnight at 4 °C in agitation; horseradish peroxidase (HPR)-conjugated secondary antibodies were diluted in blocking solution and membranes were left to incubate 2h at room temperature (RT) in agitation.

Luminescence signals were acquired with c400 Azure Molecular Imager (Aurogene). Quantitative densitometric analysis was performed with ImageJ software. When used, stripping buffer was prepared according to abcam's recipe. PCSK9 antibody (ab) was from abcam (cod. ab181142; dilution 1:1000), MGP ab was from GeneTex (cod. GTX57155; dilution 1:1000), BMP2 was from abcam (cod. ab6285, dilution 1:400), ALP was from abcam (cod. ab65834, dilution 1:500), OPN was from GeneTex (cod. GTX134553, dilution 1:1000), Sortilin was from abcam (cod. ab16640, dilution 1:1000), GAPDH ab was from GeneTex (cod. GTX100118; dilution 1:5000), anti-mouse ab was from Jackson ImmunoResearch (cod. 115-036-062; dilution 1:5000), anti-rabbit ab was from Jackson ImmunoResearch (cod. 113-036-045, dilution 1:5000).

2.3.5. Reverse transcription and quantitative PCR (RT-qPCR)

Total RNA was extracted using the iScript™ RT-qPCR Sample Prep reagent (Bio-Rad), according to the manufacturer's instructions. TranScriba 1step PCR Mix SYBR kit (A&A Biotechnology) was used for qPCR, along with specific primers for 18S (FWD 5′-CGGCTACCACATCCACGGAA-3′, REV 5′-CCTGAATTGTTATTTTTCGTCACTACC-3′) and PCSK9 (FWD 5′-CCTGCGCGTGCTCAACT-3′, REV 5′-GCTGGCTTTTCCGAATAAACTC-3′). The analyses were performed with the CFX96 Touch Real-Time PCR Detection System (Bio-Rad) with cycling conditions of 50 °C for 10 min, 95 °C for 1 min, and a repetition of 40 cycles at 95 °C for 15 s followed by 30 s at 60 °C. The data were expressed as Ct values and used for relative quantification of targets with ΔΔCt calculations. The ΔΔCt values were determined by multiplying the ratio value between the efficiency of specific primers and housekeeping 18S. The efficiency was calculated as ((10^(-1/slope)) - 1) x 100.

2.3.6. Extracellular vesicles isolation and analyses

SMCs were seeded in 100 mM dishes at cellular density of 25×10^3 cells/dish and incubated for 6 days with media supplemented with 2.5% of FBS in the presence or absence of Pi. Before extracellular vesicles (EVs) analysis, cells layer was washed twice with PBS and conditioned media were replaced with serum-free media containing 0.5% BSA for 20 h. For flow cytometry analysis, 50 μL of culture medium containing hSMCs-derived EVs were diluted with 0.22 μm-pore-size-membrane-filtered PBS 1X (Gibco) and then incubated at 37 °C in the dark for 25 min with Calcein AM (10 μM, Invitrogen) to detect intact microparticles. Afterwards, saturating concentration of monoclonal antibodies against tetraspanin family members, phycoerythrin (PE)-Cy7-conjugated CD63, peridinin phlorophyll protein complex (PerCP)-Cy5.5-conjugated CD81 and brilliant violet (BV) 421-conjugated CD9 (BD Biosciences), that are expressed by hSMCs-derived EVs, were added for 15 min at room temperature in the dark. Before use, all antibodies were centrifuged at 17,000g for 30 min at 4 °C, in order to remove any aggregate. At the end of the incubation, the samples were immediately analyzed by Gallios flow cytometer (Beckman Coulter), equipped with four solid-state lasers at 488 nm, 638 nm, 405 nm, and 561 nm, with an enhanced wide forward angle light scatter optimized for EVs detection. Flow-check Pro Fluorospheres (Beckman Coulter) were daily used to monitor cytometer performance according to the manufacturer's instruction. Megamix-SSC Plus beads (0.5, 0.9, 3 μm, BioCytex) were used to define the analysis gate and BD Trucount tubes to have the absolute count of EVs.

For Western blotting analysis, the serum free media were centrifuged (500*g* at 4 °C) for 10 min to pellet cells and subsequently the supernatant was collected and the EVs released in the media were isolated by ultracentrifugation (24,000 rpm at 4 °C for 2 h, L7-80 ultracentrifuge, Beckman Coulter), after which the media were discarded, and the EVs-containing pellets were resuspended in 100 μL of cold PBS and stored at −80 °C for further experiments. Three freezing/thawing cycles were performed to lyse the EVs.

The morphology of EVs was examined by transmission electron microscopy (TEM) using the Tecnai G2 microscope (FEI). Samples were deposited on a small holey carbon-coated support grid (400 mesh) and the solvent was allowed to dry at room temperature. Prior to TEM imaging, samples were negatively stained with 1% w/v aqueous uranyl acetate solution. TEM images were captured by rotating the sample from +60° to −60° and collected every 2° of rotation.

Numbers and dimensions of EVs were assessed by nanoparticle tracking analysis (NTA), using the NanoSight NS300 system (Malvern Panalytical Ltd.) [45], which measures the Brownian motion of particles suspended in fluid and displays them in real time through a high sensitivity CCD camera. Five 30s recordings were made for each sample.

Collected data were analyzed with NTA software (Malvern Panalytical Ltd.), which provided high-resolution particle-size distribution profiles as well as measurements of the EVs concentration.

2.3.7. Statistical analysis

Data are expressed as mean ± standard deviation. To compare differences between two conditions, p values were determined by Student's *t*-test using GraphPad® Software v8.2.1 for Windows. Otherwise, differences between treatment groups were evaluated by one-way ANOVA. A probability value of $p < 0.05$ was considered statistically significant.

3. Results

3.1. PCSK9 plasma levels increased in atherosclerotic subjects with low GFR

At univariate analysis, we observed that PCSK9 plasma levels were increased in subjects with renal dysfunction and with atherosclerotic calcification ("CKD+/ATH+", n = 104) as compared to those with renal dysfunction but without atherosclerotic calcifications ("CKD+/ATH-", n = 173) and those without renal dysfunction and without atherosclerotic calcification ("CKD-/ATH-", n = 330) (Supplemental Table 1, subjects from the PLIC study [6,46–48], see Materials and methods). Since these three groups also differed for classical cardiovascular risk factors (age, waist circumference/overweight, smoking habit, hypertension, and dyslipidemia), we then explored whether these differences in plasma PCSK9 were independently associated with renal impairment and atherosclerotic calcifications. When controlling for these risk factors, PCSK9 plasma levels were still increased in "CKD+/ATH+" *vs* "CKD+/ATH-" (339.4 ± 11.9 ng/mL *vs* 306.9 ± 8.8 ng/mL, $p = 0.007$) as well as *vs* "CKD-/ATH-" (339.4 ± 11.9 ng/mL *vs* 214.1 ± 6.6 ng/mL, $p < 0.001$) (Fig. 1), prompting us to investigate the relationship between PCSK9 and vascular calcifications in CKD.

3.2. Psck9 levels are induced in uremic rats

To investigate the relationship between PCSK9, kidney function, and vascular calcification, we adopted an *in vivo* experimental model of adenine-induced chronic kidney damage [49]. After 6 weeks, the development of a uremic condition was confirmed by a significant increase of creatinine and phosphate plasma levels (Fig. 2A and B). In addition, we observed a partial anemia with reduced hemoglobin levels and red blood cells count (Fig. 2C and D). Weights of rats fed a control diet raised from 424.7 ± 22.5 g to 563.4 ± 40.9 g (+32%) during the 6 weeks of the study, while adenine-fed rats weight decreased from 502.7 ± 73.4 g to 329.8 ± 49.7 g (−34%), showing a suffering phenotype as previously reported [50]. High phosphate levels induced a massive aortic calcification determined both by biochemical tests and von Kossa staining (Fig. 2E and F). Immunohistological analysis also confirmed the presence of Pcsk9 in medial SMCs in both control and adenine treated rats (Fig. 2F). Taken together, these observations indicate that adenine supplementation induces a uremic condition associated with a diffuse vascular calcification in response to high phosphate levels.

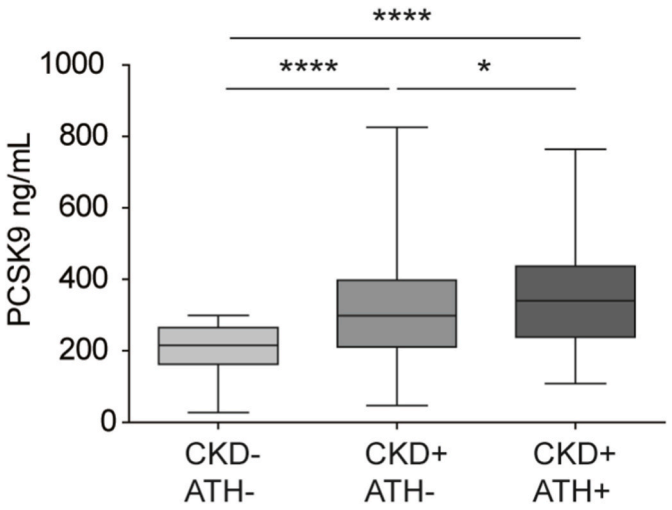

Fig. 1. PCSK9 plasma levels in subjects of the PLIC cohort depend on kidney function and atherosclerotic disease.
Serum PCSK9 level (ng/mL; mean, 95% CI) in the study population subgroups. CKD-/ATH-: subjects without CKD and atherosclerotic calcifications; CKD+/ATH-: CKD subjects without atherosclerotic calcifications; CKD+/ATH+: CKD subjects with atherosclerotic calcifications. *$p < 0.05$; ****$p < 0.0001$.

Interestingly, uremic rats showed a mild, but significant, hypercholesterolemia with an increase of total cholesterol level from 79 mg/dL to 109 mg/dL (Fig. 3A). This result is in line with what observed in a murine model of nephrotic syndrome, where the contribution of Pcsk9 to the hypercholesterolemic status has been hypothesized [51]. Therefore, we evaluated the effect of uremic status on plasma, liver, and kidney levels of Pcsk9. Uremic rats showed a significant 2.7-fold increase in plasma levels of Pcsk9 compared to controls (Fig. 3B). Western blot analysis of total protein extracts of liver and kidney also showed a mild, but not significant, increase of Pcsk9 in the liver (Fig. 3C) and a 5-fold upregulation of Pcsk9 in kidney (Fig. 3D). In conclusion, the induction of kidney failure determined a mild hypercholesterolemic status associated with a significant increase of circulating and kidney Pcsk9 levels.

3.3. PCSK9 increases SMCs calcification in response to high phosphate concentration

To investigate a possible role of PCSK9 in arterial calcification, we performed a series of *in vitro* experiments with rat and human SMCs overexpressing human PCSK9. Retroviral infection with plasmid encoding human PCSK9 determined a significant upregulation of the protein levels both in rat and human SMCs, as determined by Western blot (Fig. 4A and C) and ELISA assay (Fig. 4D), respectively. To mimic the hyperphosphatemia observed in uremic rats, we exposed control (SMCs) and PCSK9 overexpressing cells ($SMCs^{PCSK9}$) to 2.0 and 2.4 mM of Pi for 6 days. This experimental condition induced SMCs calcification, as determined by the measurement of extracellular Ca^{2+} levels (Fig. 4B and E). In particular, rat SMCs (rSMCs) seem to be more prone to calcification with a massive response also at 2.0 mM of phosphates; on the contrary, human SMCs (hSMCs) showed increased calcium deposition at 2.4 mM. Importantly, the overexpression of PCSK9 increased calcium deposition in both rat and human SMCs (Fig. 4B and E). The effect of PCSK9 was more evident in hSMCs, although these cells tend to deposit a lower amount of extracellular calcium compared to rSMCs (≈0.2 mg Ca^{2+}/mg protein *vs* ≈ 3.5 mg Ca^{2+}/mg protein for hSMCs and rSMCs, respectively). Interestingly, the addition of exogenous human recombinant PCSK9 (5 μg/mL) did not alter the *in vitro* hSMCs calcification (Fig. 4F), indicating that intracellular synthesized PCSK9 is involved in this process. Accordingly, the addition of anti PCSK9 monoclonal antibody evolocumab did not affect, but rather marginally increased, calcium deposition in $hSMCs^{PCSK9}$ (Fig. 4G). Interestingly, basal endogenous levels of PCSK9 (mRNA and protein) were significantly induced in response to increasing concentrations of simvastatin in control SMCs (Fig. 4H and I) [52].

Established evidence on the mechanisms of mineralization identified extracellular vesicles (EVs) derived from SMCs as the mediator of calcification in diseased heart valves and atherosclerotic plaques [53]. We therefore investigated a possible effect of PCSK9 on EVs released and composition by flow-cytometry, Western blot, NanoSight and electron microscopy (EM) analyses.

By flow-cytometry, we observed that the exposure of $hSMCs^{PCSK9}$ to high phosphate concentration determined a significant increase of EVs

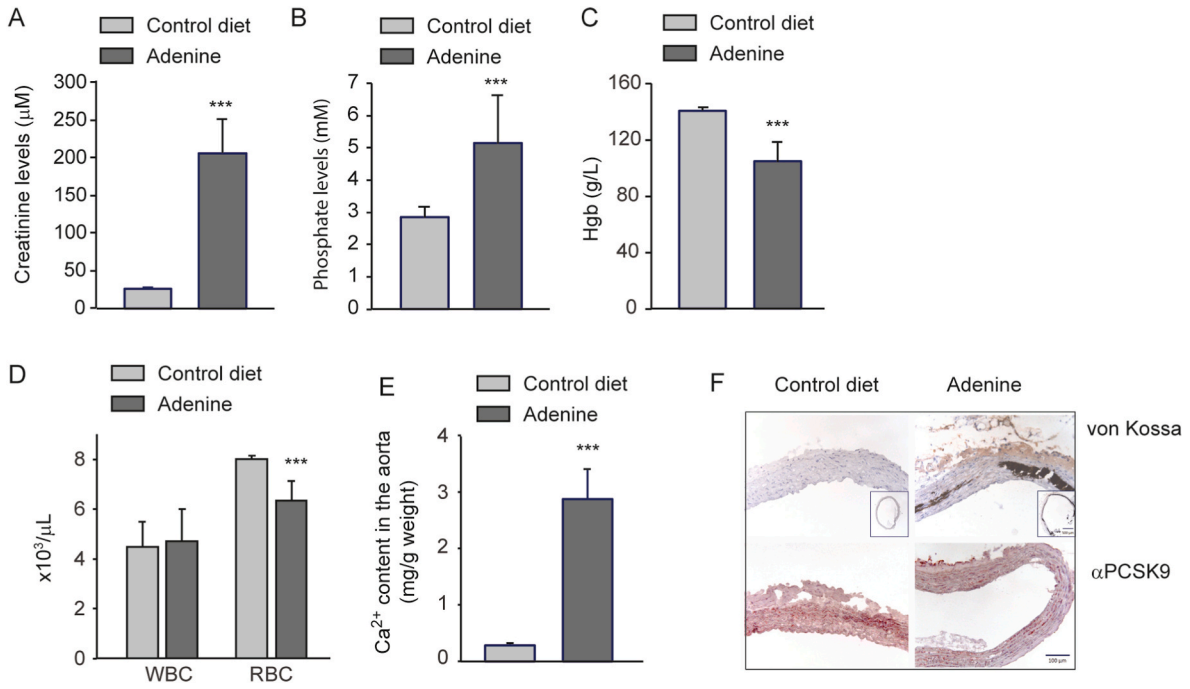

Fig. 2. Adenine-supplemented diet induces kidney failure and vascular calcification in rats.
Twenty-two rats were randomly divided into control (n = 11) and uremic group (adenine) (n = 11) and sacrificed for biochemical and histological analysis after 6 weeks. (A) Serum creatinine levels; (B) serum phosphate levels; (C) hemoglobin (Hgb) serum levels; (D) white (WBC) and red (RBC) blood cell count; (E) Ca^{2+} aortic content; (F) upper panels, von Kossa staining for calcium (dark brown); lower panels, immunohistological analysis with anti-PCSK9 antibody of aorta. ***$p < 0.001$ *vs* control. Data are presented as mean ± SD.

positive for three tetraspanin molecules, such as CD63, CD9, and CD81, compared to control hSMCs (Fig. 5A–D). Additional information about the morphology and the size of EVs present in hSMCs-conditioned media was obtained by EM and NanoSight analyses, revealing that the EVs isolated from control hSMCs appeared bigger than those from $hSMCs^{PCSK9}$ (221.0 ± 3.0 nm *vs* 198.4 ± 2.4 nm) (Fig. 5E). More importantly, EVs from $hSMCs^{PCSK9}$ have a significant higher content of Ca^{2+} (Fig. 5F) and the pro-calcific alkaline phosphatase (ALP) (Fig. 5G) than control hSMCs when exposed to 2.4 mM of Pi. Finally, we detected, by Western blot analysis, PCSK9 in EVs from $hSMCs^{PCSK9}$ (Fig. 5H).

Since sortilin, a cellular mediator of SMCs calcification [29], has been shown to directly interact with PCSK9 [30] and to mediate the *in vivo* pro-calcific effect of PCSK9 [27], we determined its expression levels in our cultured system. In both hSMCs and $hSMCs^{PCSK9}$, the exposure to phosphate determined a significant reduction of sortilin levels, however, the overexpression of PCSK9 was associated with lower intracellular sortilin expression even under basal conditions (Fig. 5I).

A critical role in the initiation and progression of vascular calcification during elevated phosphate conditions is attributed to vascular SMCs, which are able to change their phenotype into osteo/chondroblasts like cells. Thus, to further unravel the "pro-calcific" PCSK9 action in SMCs, we analyzed the expression of different players of vascular calcification in response to high-phosphate concentrations.

As documented in EVs analysis, intracellular levels of ALP were also partially increased in $hSMCs^{PCSK9}$ compared to control hSMCs after exposure to 2.0 and 2.4 mM of Pi (Fig. 6A and B). A second pro-calcific factor, the bone morphogenetic protein 2 (BMP2), was increased by two-fold in $hSMCs^{PCSK9}$ compared to hSMCs when exposed to 2.4 mM Pi (Fig. 6A and C). Together with these changes, a significant reduction of the inhibitor of arterial calcification matrix GLA protein (MGP) was observed in $hSMCs^{PCSK9}$, while minor changes were observed for osteopontin (OPN) (Fig. 6A, D and 6E). In particular, MGP expression was reduced by 60% in $hSMCs^{PCSK9}$ compared to hSMCs after exposure to 2.4 mM Pi. In su mMary, the overexpression of PCSK9 directly modulate the expression of key players of arterial calcification that may contribute to the increase of hSMCs calcification observed *in vitro*.

4. Discussion

In the present study, we have investigated a possible direct role of PCSK9 on vascular calcification associated with CKD. The analysis of PCSK9 plasma levels in subjects with GFR above 70 mL/min and below 60 mL/min revealed that kidney function influences PCSK9 metabolic fate in humans. Thus, low GFR is associated with higher PCSK9 plasma levels, that increase even more significantly in patients with GFR <60 mL/min and with advanced atherosclerotic plaque disease. A similar trend was observed also in statin-treated patients, who have higher PCSK9 plasma levels compared to patients not under statin regimen (data not shown). Although a clear effect on PCSK9 levels has been documented in nephrotic syndrome or peritoneal dialysis [18], the effect of CKD do not seem to be consistent [15,16]. This may be explained by the population analyzed in these studies and by the size of the cohort. We have recently analyzed 3673 out of 3703 individuals of the IMPROVE European cohort and demonstrated, by multivariate analysis, a "suggestive" association between GFR and PCSK9 level [17], although most of these subjects had normal kidney function (GFR above 70 mL/min).

In animal models of nephrotic syndrome, a significant increase of Pcsk9 hepatic synthesis has been documented. Similarly, we have reported that uremic rats showed slightly higher Pcsk9 protein levels in the liver and a significant 2.7-fold increase in the kidney compared to control rats [49]. These data suggest a possible increase of PCSK9 synthesis by both liver and kidney (or other sources), which resulted in higher circulating PCSK9 levels and mild increase of plasma total cholesterol. PCSK9 is mainly regulated at the transcriptomic level, and it is highly upregulated in response to partial hepatectomy [54]. Thus, it is possible that, in our model, Pcsk9 was induced in response to kidney dysfunction, as observed in response to renal ischemia/reperfusion rats [55]. In addition, we speculate that the increase in total cholesterol plasma levels in our model is probably driven by raised plasma Pcsk9 of

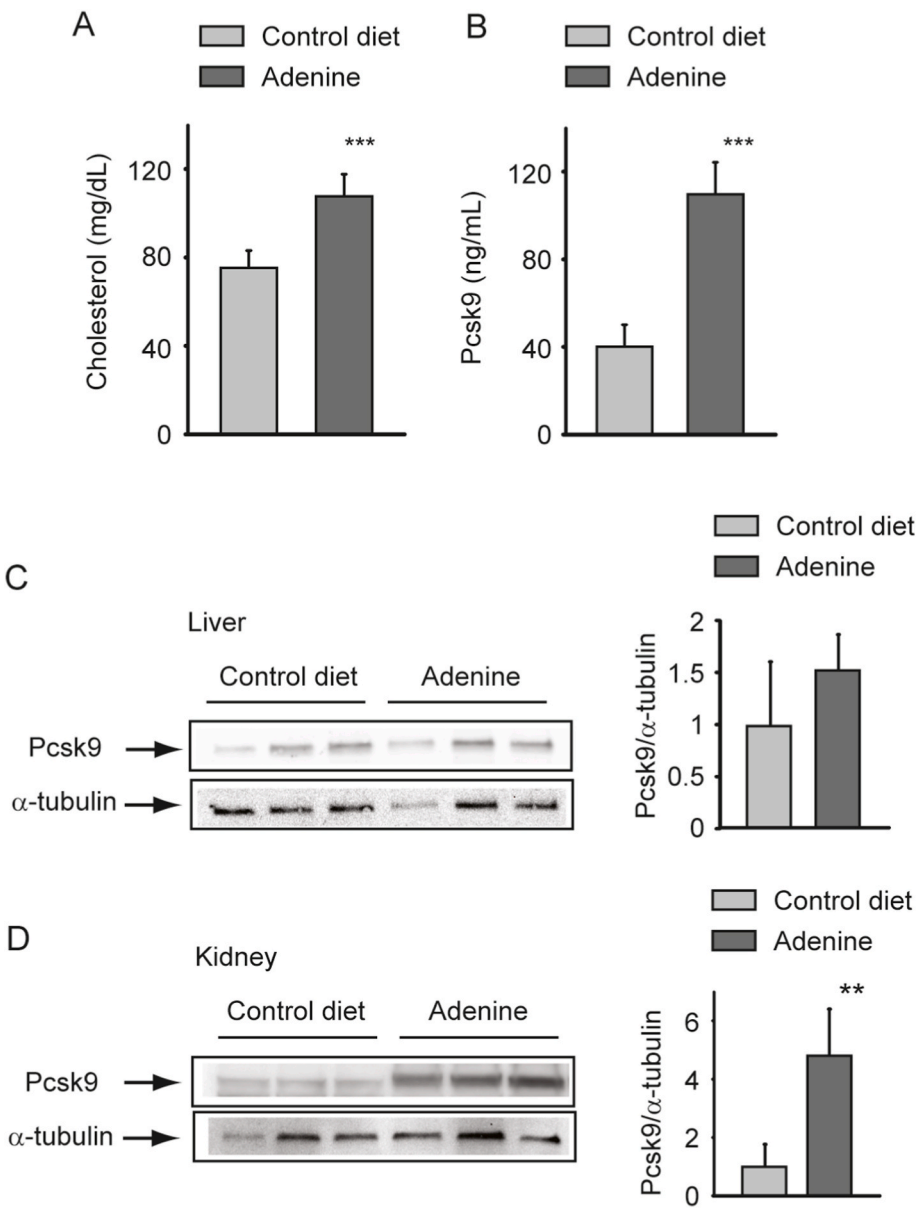

Fig. 3. Pcsk9 levels increased in uremic rats.
(A) Total cholesterol was determined from sera of both control and uremic rats (adenine) with a colorimetric assay (Horiba); (B) from the same serum samples, Pcsk9 concentrations were determined with the ELISA assay; total protein extracts from liver (C) and kidney (D) were analyzed by Western blot with anti-Pcsk9 antibody. α-tubulin was used as loading control. The right panels show the optical quantification of the Western blot analysis. $^{**}p < 0.01$ *vs* control. Data are presented as mean ± SD of 6 animals per group.

kidney origin. This hypothesis is supported by the observation of increased PCSK9 levels in mice model of focal and segmental glomerulosis [56]. Moreover, a selective deletion of Pcsk9 in the renal collecting duct failed to develop hypercholesterolemia upon injection of nephrotoxic serum, once more suggesting the renal origin of plasma PCSK9 [56]. Nevertheless, the contribution of other organs to Pcsk9 plasma levels cannot be excluded.

In our *in vivo* model of adenine-induced uremic rats, we observed an extensive vascular calcification probably due to hyperphosphatemia. Within this vascular response we speculated that PCSK9 might play a role since it is extensively expressed in aorta SMCs [35]. In addition, we have previously reported that: (1) old *Pcsk9* null mice had lower aortic valve calcification than wild-type mice; (2) *Pcsk9* null vascular interstitial cells were partially protected from *in vitro* calcification; (3) PCSK9 is highly expressed in human calcified aortic valves; and (4) human aortic valve calcification might be caused by vascular interstitial cell-related PCSK9 expression [57]. To extend these observations, we moved to an *in vitro* model where we generated both rat and human SMCs overexpressing PCSK9 and determined cellular calcification in response to high phosphate concentrations. Both human and rat SMCs showed a significantly higher extracellular calcium when PCSK9 was overexpressed. In human SMCs overexpressing PCSK9, the amount of PCSK9 detected in the extracellular compartment was approximately 11 ng/mL. The addition of 5 μg/mL of human recombinant PCSK9 did not change the calcification process in cultured human SMCs. The amount of PCSK9 was used according to results of our and other previous *in vitro* studies that demonstrated the requirement of at least 5 μg/mL in order to induce the degradation of the LDL receptor [35,58]. These data bring us to speculate that intracellular PCSK9 drives the *in vitro* calcification. This hypothesis may be corroborated by the evidence that, under our experimental settings, evolocumab did not affect the extracellular calcium deposition both in hSMCs and $hSMCs^{PCSK9}$.

In response to elevated phosphate conditions, SMCs undergo an osteogenic switch and secrete EVs that are heterogeneous in terms of their origin and composition [59,60]. Physiologically, EVs contain high levels of calcification inhibitors, such OPN as MGP, while under pathological conditions, and particularly in the presence of uremic toxins, the secreted EVs acquire a pro-calcifying profile and thereby act as nucleating foci for the crystallization of hydroxyapatite and the propagation of calcification [53]. Our *in vitro* analyses documented that the

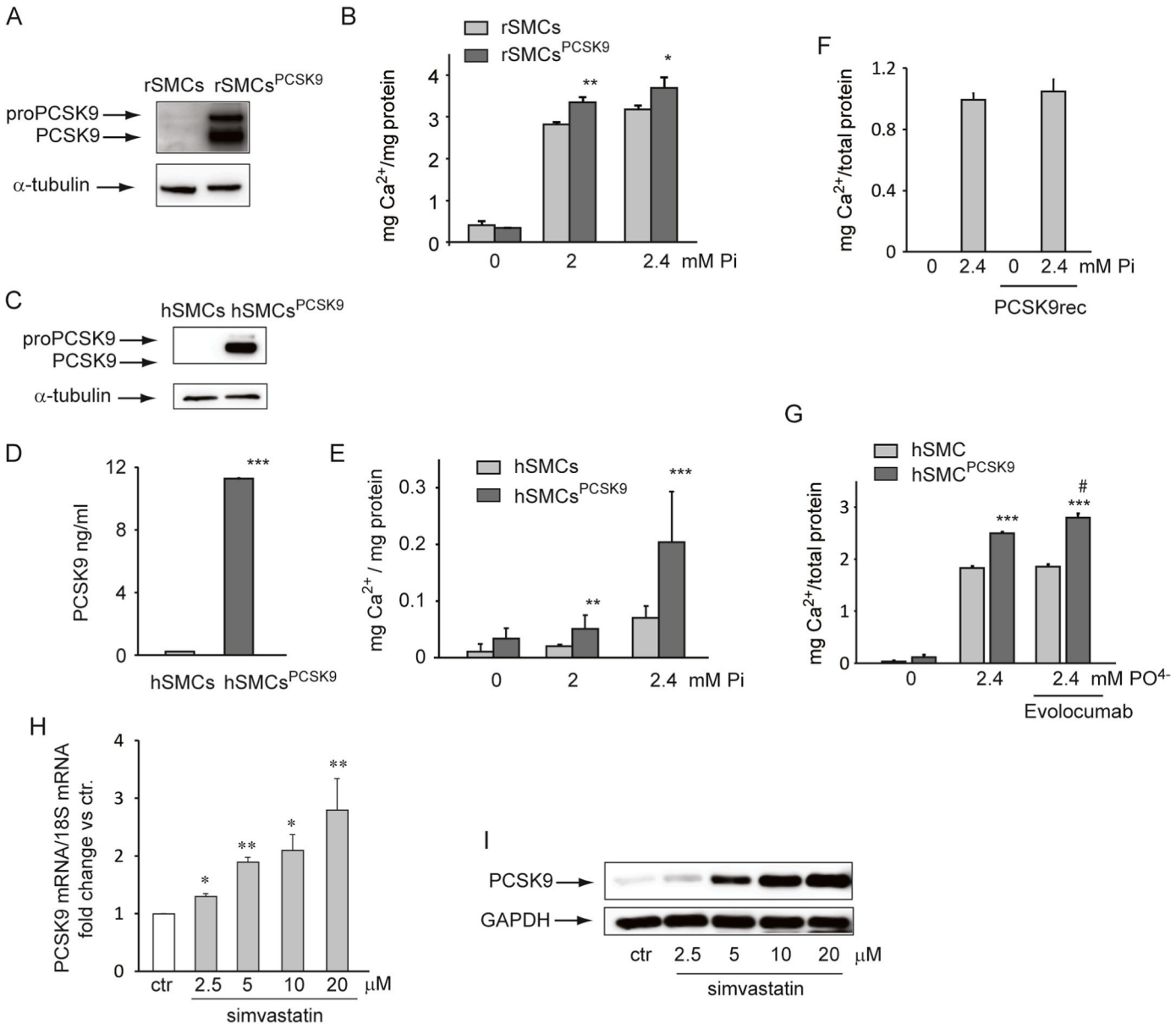

Fig. 4. PCSK9 overexpression induces SMC calcification *in vitro*.
Rat and human SMCs were retrovirally transduced with empty and PCSK9 encoding vector and after puromycin selection, PCSK9 levels were determined by Western blot analysis (A and C) and ELISA assay (D). (B and E) SMCs control and overexpressing PCSK9 ($SMCs^{PCSK9}$) were cultured in DMEM/2.5% FCS in the presence or absence of the indicated concentrations of phosphate (P_i) for 6 days. At the end of the incubation, the extracellular concentrations of Ca^{2+} were determined withy colorimetric assay and normalized to total cellular protein content. (F) SMCs were incubated in DMEM/2.5% FCS in the presence or absence of 2.4 mM P_i and 5 μg/mL of recombinant human PCSK9 (PCSK9rec). (G) Under the same experimental conditions described for panel E, human SMCs control and $SMCs^{PCSK9}$ were incubated with evolocumab (10 μg/mL). (H and I) SMCs were incubated with the indicated concentrations of simvastatin for 24h and mRNA (H) or protein (I) expression determined by qPCR and Western blot analysis with anti-PCSK9 antibody, respectively. GAPDH was used as loading control. After 6 days, extracellular concentrations of Ca^{2+} were determined. *$p < 0.01$; **$p < 0.01$; ***$p < 0.0001$ SMCs *vs* SMC^{PCSK9}. rSMCs: rat SMCs; hSMCs: human SMCs.

overexpression of PCSK9 in hSMCs determined a significant reduction of calcification inhibitors MGP and OPN and a concomitant induction of pro-calcific factor, such as ALP and BMP2. BMP2 signaling promotes the expression of osteoblast lineage markers including ALP and the osteoblast/chondrocyte master transcriptional regulator RUNX2 inducing the mineralization of cultured human coronary vascular SMCs [61,62]. The role of PCSK9 on vascular cells differentiation has been previously reported [63]. More recently, PCSK9 was shown to mediates vascular SMCs apoptosis and senescence [64], a phenomenon strictly implicated in vascular calcification process through a transition towards to an osteoblastic phenotype [65]. The effect of PCSK9 on senescence and apoptosis seems to be mediated by ApoER2 downregulation [64]. From this evidence, it is tempting to speculate a role for ApoER2 on PCSK9-mediated vascular calcification.

The positive effect of PCSK9 on osteogenic and pro-calcific phenotype was also supported by the fact that, in response to high phosphate concentrations, $hSMCs^{PCSK9}$ increased their capability to release $CD63^{-}$, $CD9^{-}$and $CD81^{-}$positive EVs. EVs derived from $hSMCs^{PCSK9}$ showed also a significantly higher calcium and ALP content, factors that may certainly contribute to SMCs calcification process. The role of PCSK9 on the EVs formation is also supported by the observation of a direct protein-protein interaction between PCSK9 and sortilin [30], a cellular mediator of SMC calcification [29]. In addition, the lack of sortilin was shown to significantly reduce the procalcific effect of Pcsk9 in mice [27].

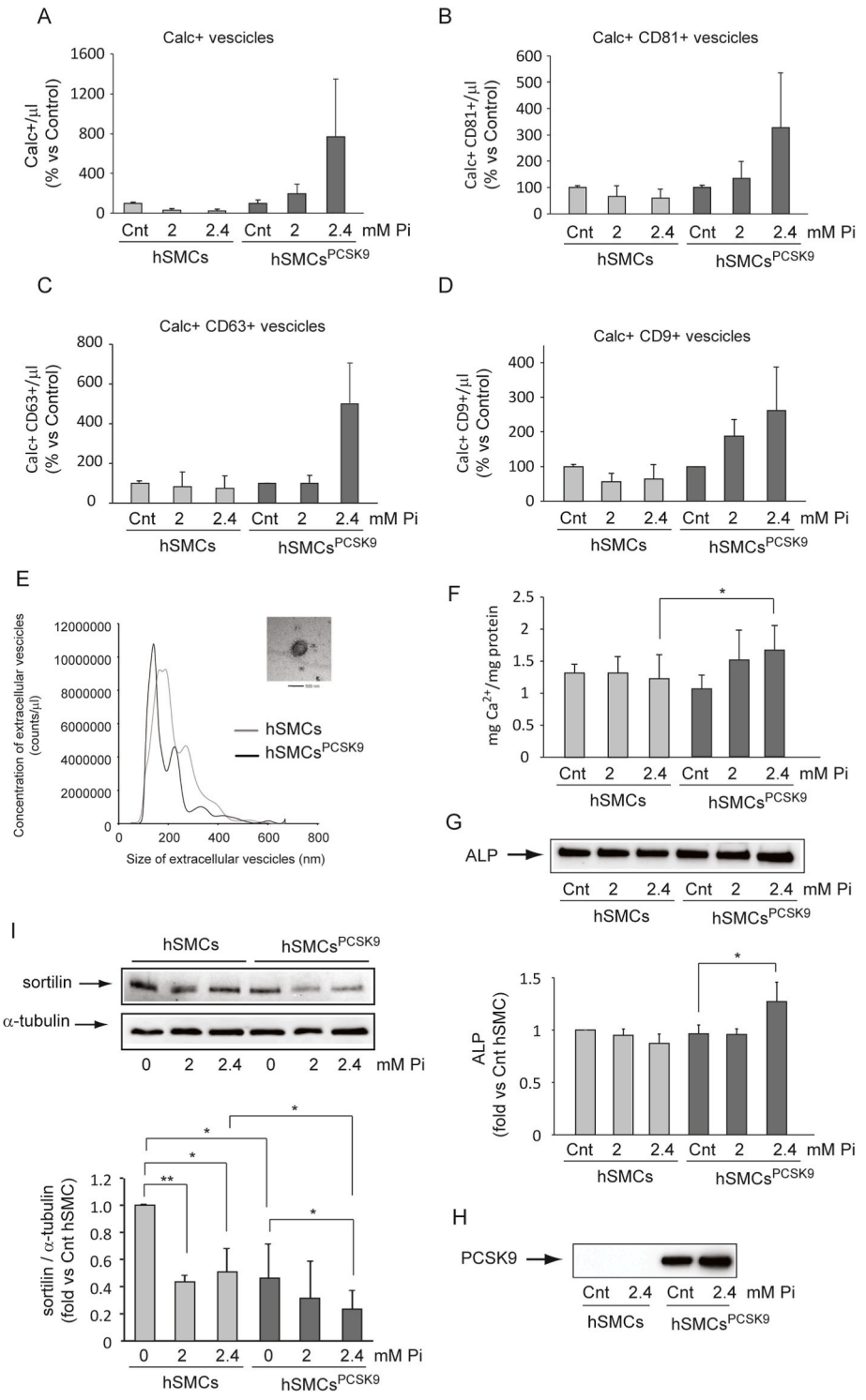

Fig. 5. Extracellular vesicles characterization of SMCs and SMCs^{PCSK9}.
(A–D) Human SMCs and SMCs^{PCSK9} were cultured in DMEM in the presence or absence of the indicated concentrations of phosphate (P_i) for 6 days. At the end of the incubation, the conditioned media were collected and analyzed by flow cytometry after labelling with Calcein (Calc+) (A) in combination with anti-CD81 (B) anti-CD63 (C) and anti-CD9 (D) antibodies. (E) Under the same experimental conditions of panels A–D, EVs from SMCs were analyzed by electron microscopy (insert panel) and by NanoSight. (F) EVs were collected by ultracentrifugation and Ca^{2+} content was determined by colorimetric assay and normalized to total protein content. (G) EVs protein extracts were analyzed by Western blot with anti-alkaline phosphatase (ALP) antibodies. The graph shows the densitometric analysis of three independent experiments assessing ALP. (H) PCSK9 detection by Western blotting analysis from EVs protein extracts. (I) Under the same experimental conditions of panels A–D, at the end of the incubation, total protein extracts were prepared and analyzed by Western blot with antibodies anti-sortilin. α-tubulin was used as loading control. Differences between treatments were assessed by Student's *t*-test and one-way ANOVA (when necessary). $^{*}p < 0.05$; $^{**}p < 0.01$.

All these evidence suggest that intracellular PCSK9 may induce the release of vesicles involved in SMCs calcification [66]. Indeed, the addition of recombinant human PCSK9 did not produce any effect on SMCs calcification in our *in vitro* model. From these considerations, we have studied sortilin expression and found that hSMCs^{PCSK9} have lower levels of this pro-calcific factor compared to control hSMCs. A possible interpretation of this observation could be related to the presence of sortilin inside the EVs [29] that are more efficiently released by hSMCs overexpressing PCSK9.

Finally, we provide evidence that PCSK9 is present in EVs when overexpressed in SMCs. This observation could be pathophysiological relevant considering that: (1) PCSK9 has been found enriched in caveolin-endosomes via a cyclase-associated protein 1 (CAP1)-mediated interaction [67], and caveolin-1 is a component of procalcific EVs both during bone mineralization [68] and calcification of the vascular wall [29], (2) annexin A2 is a natural inhibitor of PCSK9 [69], a protein found to be reduced in EVs upon VSCMs Ca^{2+} overload [70]. These observations may reinforce our hypothesis on a direct role for PCSK9 in vascular calcification, although additional studies should be performed to investigate the molecular mechanisms.

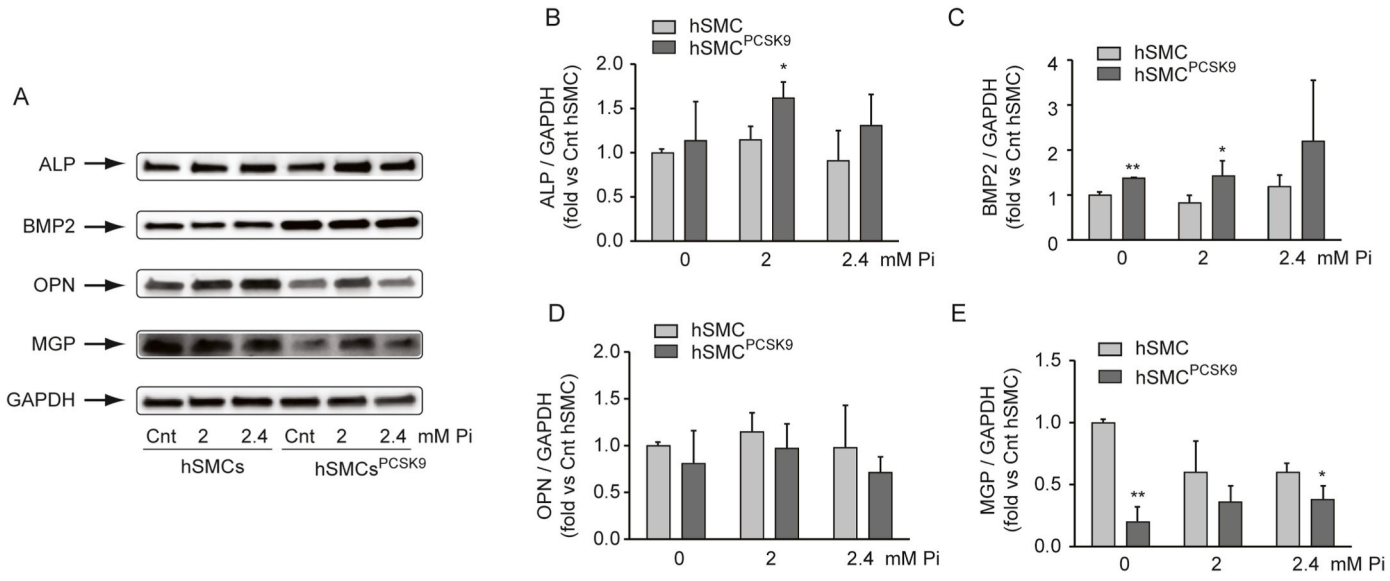

Fig. 6. PCSK9 induces SMCs differentiation into a pro-calcific phenotype.
Human SMCs and SMCs^{PCSK9} were cultured in DMEM in the presence or absence of the indicate concentrations of phosphate (P_i) for 6 days. At the end of the incubation, total protein extracts were prepared and analyzed by Western blot with antibodies anti-alkaline phosphatase (ALP), bone morphogenic protein 2 (BMP2), osteopontin (OPN) and matrix GLA protein (MGP). GAPDH was used as loading control. (A) Representative captures. (B–E) Western blot densitometric analysis of three independent experiments assessing ALP (B), BMP (C), OPN (D) and MGP (E) protein levels. Differences between treatments were assessed by Student's t-test. *$p < 0.05$; **$p < 0.01$; ***$p < 0.001$ hSMCs *vs* hSMC^{PCSK9}.

In conclusion, our data suggest a major role for PCSK9 in vascular calcification, with a possible direct involvement of SMCs intracellular PCSK9 rather than circulating ones. Thus, the increased plasma levels of PCSK9 observed in patients with GFR <60 mL/min and with advanced atherosclerotic plaque disease may be related to impaired kidney function as also recently observed in the European cohort of the IMPROVE study [17]. Plasma PCSK9 is mainly from hepatic origin, however, the use of inclisiran, a small interfering RNA (siRNA) designed to target PCSK9 mRNA exclusively in the liver [71], brought to ≈70% reduction of plasma PCSK9, thus implying that 30% of its amount is from extrahepatic tissues, including the vasculature [35]. Thus, it is still unknown whether circulating PCSK9 is simply a biomarker of atherosclerotic plaque disease or a direct player of the pathology, and if the different source of PCSK9 (liver, kidney, and vasculature) have a peculiar pathophysiological role. Indeed, while a number of studies did not report an association between PCSK9 levels and cardiovascular events [72–74], different conclusions were reached by others [75–78]. Thus, this topic will warrant much attention in the future also considering that PCSK9 may circulate as free or lipoprotein-bound, and as furin-cleaved forms. Even more intriguingly, it will be interesting to determine if PCSK9 is detected in extracellular vescicles in human plasma considering our *in vitro* observation.

In addition, it is tempting to speculate that increased progression of coronary and aortic calcification induced by 3-hydroxy-3-methylglutaryl-CoA (HMG-CoA) reductase inhibitors (statins) [79–81], may be related to the induction of intracellular PCSK9 by this class of drug. However, the monoclonal antibodies anti PCSK9 (evolocumab), did not affect the extracellular calcium deposition in our *in vitro* cultured model, in accordance with the clinical data of the GLAGOV study [26]. Indeed, anti PCSK9 monoclonal antibodies and inclisiran, which is designed to target PCSK9 mRNA exclusively in the liver [71], may have a minimal inhibitory capacity on intracellular PCSK9 in vascular SMCs [82]. On the contrary, a classical pharmacological approach with small chemical entities with anti-PCSK9 activity may produce a protective effect on vascular calcification. This hypothesis might be tested for instance with small molecules anti-PCSK9, currently in clinical development [83,84].

Financial support

This work was supported by Ministero dell'Istruzione, dell'Università e della Ricerca, project PRIN 2017 (CUP C94I19002530001). The work of ALC and AB was supported by Ministry of Health - Ricerca Corrente - IRCCS MultiMedica and "Cibo, Microbiota, Salute" by "Vini di Batasiolo S.p.A" AL_RIC19ABARA_01 to A.B., "Post-Doctoral Fellowship 2020" by "Fondazione Umberto Veronesi" 2020–3318 to A.B. The work was also supported by a funding of the Russian Ministry of Science and Higher Education (Agreement No. 075-15-2020-901 dated November 13, 2020).

Declaration of competing interests

The authors declare that they have no known competing financial interests or personal relationships that could have appeared to influence the work reported in this paper.

CRediT authorship contribution statement

Maria Giovanna Lupo: contributed to the interpretation of data, Formal analysis. **Alessandro Bressan:** contributed to the interpretation of data, Formal analysis. **Maristella Donato:** Formal analysis. **Paola Canzano:** Formal analysis. **Marina Camera:** contributed to the conception, design of the work, Writing – original draft. **Paolo Poggio:** contributed to the conception, design of the work, Writing – original draft. **Maria Francesca Greco:** contributed to the acquisition and analysis of data. **Mariangela Garofalo:** Formal analysis. **Sara De Martin:** contributed to the interpretation of data. **Giovanni Panighel:** Formal analysis. **Massimiliano Ruscica:** contributed to the conception, design of the work, Writing – original draft, contributed to the interpretation of data. **Andrea Baragetti:** contributed to the interpretation of data, Formal analysis. **Valentina Bollati:** contributed to the interpretation of data. **Elisabetta Faggin:** Formal analysis. **Marcello Rattazzi:** contributed to the conception, design of the work, Writing – original draft, contributed to the interpretation of data. **Alberico L. Catapano:** contributed to the conception, design of the work, Writing – original draft. **Nicola Ferri:** contributed to the conception, design of the work,

Writing – original draft, All gave final approval and agreed to be accountable for all aspects of work ensuring integrity and accuracy.

Appendix A. Supplementary data

Supplementary data to this article can be found online at https://doi.org/10.1016/j.atherosclerosis.2022.01.015.

References

[1] R.T. Gansevoort, R. Correa-Rotter, B.R. He mMelgarn, et al., Chronic kidney disease and cardiovascular risk: epidemiology, mechanisms, and prevention, Lancet 382 (2013) 339–352.

[2] C. Chronic Kidney Disease Prognosis, K. Matsushita, M. van der Velde, et al., Association of estimated glomerular filtration rate and albuminuria with all-cause and cardiovascular mortality in general population cohorts: a collaborative meta-analysis, Lancet 375 (2010) 2073–2081.

[3] A.S. Go, G.M. Chertow, D. Fan, et al., Chronic kidney disease and the risks of death, cardiovascular events, and hospitalization, N. Engl. J. Med. 351 (2004) 1296–1305.

[4] G.M. London, A.P. Guerin, S.J. Marchais, et al., Arterial Media Calcification in End-Stage Renal Disease: Impact on All-Cause and Cardiovascular Mortality, Nephrology, Dialysis, Transplantation : Official Publication of the European Dialysis and Transplant Association, 18, European Renal Association, 2003, pp. 1731–1740.

[5] M. Schoppet, R.C. Shroff, L.C. Hofbauer, et al., Exploring the biology of vascular calcification in chronic kidney disease: what's circulating? Kidney Int. 73 (2008) 384–390.

[6] A. Baragetti, G.D. Norata, C. Sarcina, et al., High density lipoprotein cholesterol levels are an independent predictor of the progression of chronic kidney disease, J. Intern. Med. 274 (2013) 252–262.

[7] I. Mikolasevic, M. Zutelija, V. Mavrinac, et al., Dyslipidemia in patients with chronic kidney disease: etiology and management, Int. J. Nephrol. Renovascular Dis. 10 (2017) 35–45.

[8] S. Sudhakaran, T. Bottiglieri, K.M. Tecson, et al., Alteration of lipid metabolism in chronic kidney disease, the role of novel antihyperlipidemic agents, and future directions, Rev. Cardiovasc. Med. 19 (2018) 77–88.

[9] F. Kronenberg, Causes and consequences of lipoprotein(a) abnormalities in kidney disease, Clin. Exp. Nephrol. 18 (2014) 234–237.

[10] H. Konishi, K. Miyauchi, S. Tsuboi, et al., Plasma lipoprotein(a) predicts major cardiovascular events in patients with chronic kidney disease who undergo percutaneous coronary intervention, Int. J. Cardiol. 205 (2016) 50–53.

[11] N.G. Seidah, A. Prat, A. Pirillo, et al., Novel strategies to target proprotein convertase subtilisin kexin 9: beyond monoclonal antibodies, Cardiovasc. Res. 115 (2019) 510–518.

[12] D.M. Charytan, M.S. Sabatine, T.R. Pedersen, et al., Efficacy and safety of evolocumab in chronic kidney disease in the FOURIER trial, J. Am. Coll. Cardiol. 73 (2019) 2961–2970.

[13] A. Baragetti, G. Balzarotti, L. Grigore, et al., PCSK9 deficiency results in increased ectopic fat accumulation in experimental models and in humans, European J. Prev. Cardiol. 24 (2017) 1870–1877.

[14] L. Da Dalt, M. Ruscica, F. Bonacina, et al., PCSK9 deficiency reduces insulin secretion and promotes glucose intolerance: the role of the low-density lipoprotein receptor, Eur. Heart J. 40 (2019) 357–368.

[15] M. Morena, C. Le May, L. Chenine, et al., Plasma PCSK9 concentrations during the course of nondiabetic chronic kidney disease: relationship with glomerular filtration rate and lipid metabolism, J. Clin. Lipidol. 11 (2017) 87–93.

[16] K.S. Rogacev, G.H. Heine, G. Silbernagel, et al., PCSK9 plasma concentrations are independent of GFR and do not predict cardiovascular events in patients with decreased GFR, PLoS One 11 (2016), e0146920.

[17] N. Ferri, M. Ruscica, D. Coggi, et al., Sex-specific predictors of PCSK9 levels in a European population: the IMPROVE study, Atherosclerosis 309 (2020) 39–46.

[18] K. Jin, B.S. Park, Y.W. Kim, et al., Plasma PCSK9 in nephrotic syndrome and in peritoneal dialysis: a cross-sectional study, Am. J. Kidney Dis. : Off J. Nat. Kid. Found. 63 (2014) 584–589.

[19] T.A. Ikizler, N.J. Cano, H. Franch, et al., Prevention and treatment of protein energy wasting in chronic kidney disease patients: a consensus statement by the International Society of Renal Nutrition and Metabolism, Kidney Int. 84 (2013) 1096–1107.

[20] R. Alonso, P. Mata, O. Muniz, et al., PCSK9 and lipoprotein (a) levels are two predictors of coronary artery calcification in asymptomatic patients with familial hypercholesterolemia, Atherosclerosis 254 (2016) 249–253.

[21] W.G. Wang, Y.F. He, Y.L. Chen, et al., Proprotein convertase subtilisin/kexin type 9 levels and aortic valve calcification: a prospective, cross sectional study, J. Int. Med. Res. 44 (2016) 865–874.

[22] A. Langsted, B.G. Nordestgaard, M. Benn, et al., PCSK9 R46L loss-of-function mutation reduces lipoprotein(a), LDL cholesterol, and risk of aortic valve stenosis, J. Clin. Endocrinol. Metab. 101 (2016) 3281–3287.

[23] N. Perrot, V. Valerio, D. Moschetta, et al., Genetic and in vitro inhibition of PCSK9 and calcific aortic valve stenosis, JACC. Basic Translat. Sci. 5 (2020) 649–661.

[24] B.A. Bergmark, M.L. O'Donoghue, S.A. Murphy, et al., An exploratory analysis of proprotein convertase subtilisin/kexin type 9 inhibition and aortic stenosis in the FOURIER trial, JAMA cardiology 5 (2020) 709–713.

[25] Y. Ikegami, I. Inoue, K. Inoue, et al., The annual rate of coronary artery calcification with combination therapy with a PCSK9 inhibitor and a statin is lower than that with statin monotherapy, NPJ. Aging. Mech. Dis. 4 (2018) 7.

[26] S.J. Nicholls, R. Puri, T. Anderson, et al., Effect of evolocumab on coronary plaque composition, J. Am. Coll. Cardiol. 72 (2018) 2012–2021.

[27] C. Goettsch, J.D. Hutcheson, S. Hagita, et al., A single injection of gain-of-function mutant PCSK9 adeno-associated virus vector induces cardiovascular calcification in mice with no genetic modification, Atherosclerosis 251 (2016) 109–118.

[28] K. Musunuru, A. Strong, M. Frank-Kamenetsky, et al., From noncoding variant to phenotype via SORT1 at the 1p13 cholesterol locus, Nature 466 (2010) 714–719.

[29] C. Goettsch, J.D. Hutcheson, M. Aikawa, et al., Sortilin mediates vascular calcification via its recruitment into extracellular vesicles, J. Clin. Invest. 126 (2016) 1323–1336.

[30] C. Gustafsen, M. Kjolby, M. Nyegaard, et al., The hypercholesterolemia-risk gene SORT1 facilitates PCSK9 secretion, Cell Metabol. 19 (2014) 310–318.

[31] P. Poggio, P. Songia, L. Cavallotti, et al., PCSK9 involvement in aortic valve calcification, J. Am. Coll. Cardiol. (2018) (In press).

[32] A. Bakhshian Nik, J.D. Hutcheson, E. Aikawa, Extracellular vesicles as mediators of cardiovascular calcification, Front. Cardiovascular Med. 4 (2017) 78.

[33] P. Lanzer, M. Boehm, V. Sorribas, et al., Medial vascular calcification revisited: review and perspectives, Eur. Heart J. 35 (2014) 1515–1525.

[34] J. Voelkl, F. Lang, K.U. Eckardt, et al., Signaling pathways involved in vascular smooth muscle cell calcification during hyperphosphatemia, Cell. Mol. Life Sci. 76 (2019) 2077–2091.

[35] N. Ferri, G. Tibolla, A. Pirillo, et al., Proprotein convertase subtilisin kexin type 9 (PCSK9) secreted by cultured smooth muscle cells reduces macrophages LDLR levels, Atherosclerosis 220 (2012) 381–386.

[36] Y. Iida, H. Tanaka, H. Sano, et al., Ectopic expression of PCSK9 by smooth muscle cells contributes to aortic dissection, Ann. Vasc. Surg. 48 (2018) 195–203.

[37] A.L. Fracanzani, G. Pisano, D. Consonni, et al., Epicardial adipose tissue (EAT) thickness is associated with cardiovascular and liver damage in nonalcoholic fatty liver disease, PLoS One 11 (2016), e0162473.

[38] V. Diwan, A. Mistry, G. Gobe, et al., Adenine-induced chronic kidney and cardiovascular damage in rats, J. Pharmacol. Toxicol. Methods 68 (2013) 197–207.

[39] G. Bollee, J. Harambat, A. Bensman, et al., Adenine phosphoribosyltransferase deficiency, Clin. J. Am. Soc. Nephrol. 7 (2012) 1521–1527.

[40] J. Harambat, G. Bollee, M. Daudon, et al., Adenine phosphoribosyltransferase deficiency in children, Pediatr. Nephrol. 27 (2012) 571–579.

[41] http://gpower.hhu.de.

[42] A. Corsini, M. Bonfatti, P. Quarato, et al., Effect of the new calcium antagonist lercanidipine and its enantiomers on the migration and proliferation of arterial myocytes, J. Cardiovasc. Pharmacol. 28 (1996) 687–694.

[43] C. Macchi, M.F. Greco, M. Botta, et al., Leptin, Resistin, and Pcsk9 - the role of Stat3, Am. J. Pathol. (2020).

[44] N. Ferri, G. Colombo, C. Ferrandi, et al., Simvastatin reduces MMP1 expression in human smooth muscle cells cultured on polymerized collagen by inhibiting Rac1 activation, Arterioscler. Thromb. Vasc. Biol. 27 (2007) 1043–1049.

[45] F. Rota, L. Ferrari, M. Hoxha, et al., Blood-derived extracellular vesicles isolated from healthy donors exposed to air pollution modulate in vitro endothelial cells behavior, Sci. Rep. 10 (2020) 20138.

[46] A. Baragetti, A. Ossoli, A. Strazzella, et al., Low plasma Lecithin: cholesterol Acyltransferase (LCAT) concentration predicts chronic kidney disease, J. Clin. Med. 9 (2020).

[47] A. Baragetti, G. Pisano, C. Bertelli, et al., Subclinical atherosclerosis is associated with Epicardial Fat Thickness and hepatic steatosis in the general population, Nutrition, metabolism, and cardiovascular diseases, Nutr. Metabol. Cardiovasc. Dis. 26 (2016) 141–153.

[48] E. Olmastroni, A. Baragetti, M. Casula, et al., Multilevel models to estimate carotid intima-media thickness curves for individual cardiovascular risk evaluation, Stroke 50 (2019) 1758–1765.

[49] M.G. Lupo, N. Biancorosso, E. Brilli, et al., Cholesterol-lowering action of a novel nutraceutical combination in uremic rats: insights into the molecular mechanism in a hepatoma cell line, Nutrients (2020) 12.

[50] S. Yamada, M. Tokumoto, N. Tatsumoto, et al., Phosphate overload directly induces systemic infla mMation and malnutrition as well as vascular calcification in uremia, Am. J. Physiol. Ren. Physiol. 306 (2014) F1418–F1428.

[51] M.E. Haas, A.E. Levenson, X. Sun, et al., The role of proprotein convertase subtilisin/kexin type 9 in nephrotic syndrome-associated hypercholesterolemia, Circulation 134 (2016) 61–72.

[52] N. Ferri, S. Marchiano, M.G. Lupo, et al., Geranylgeraniol prevents the simvastatin-induced PCSK9 expression: role of the small G protein Rac1, Pharmacol. Res. 122 (2017) 96–104.

[53] J.B. Krohn, J.D. Hutcheson, E. Martinez-Martinez, et al., Extracellular vesicles in cardiovascular calcification: expanding current paradigms, J. Physiol. 594 (2016) 2895–2903.

[54] A. Zaid, A. Roubtsova, R. Essalmani, et al., Proprotein convertase subtilisin/kexin type 9 (PCSK9): hepatocyte-specific low-density lipoprotein receptor degradation and critical role in mouse liver regeneration, Hepatology 48 (2008) 646–654.

[55] C. Barisione, D. Verzola, S. Garibaldi, et al., Renal ischemia/reperfusion early induces myostatin and PCSK9 expression in rat kidneys and HK-2 cells, Int. J. Mol. Sci. (2021) 22.

[56] E. Molina-Jijon, S. Gambut, C. Mace, et al., Secretion of the epithelial sodium channel chaperone PCSK9 from the cortical collecting duct links sodium retention with hypercholesterolemia in nephrotic syndrome, Kidney Int. 98 (2020) 1449–1460.

[57] P. Poggio, P. Songia, L. Cavallotti, et al., PCSK9 involvement in aortic valve calcification, J. Am. Coll. Cardiol. 72 (2018) 3225–3227.
[58] T.A. Lagace, D.E. Curtis, R. Garuti, et al., Secreted PCSK9 decreases the number of LDL receptors in hepatocytes and in livers of parabiotic mice, J. Clin. Invest. 116 (2006) 2995–3005.
[59] L.M. Doyle, M.Z. Wang, Overview of extracellular vesicles, their origin, composition, purpose, and methods for exosome isolation and analysis, Cells 8 (2019).
[60] A. Tanimura, T. Cho, S. Tanaka, Aortic changes induced by hypercholesterolemia and hypercalcemia in rats, Exp. Mol. Pathol. 44 (1986) 297–306.
[61] P.B. Yu, D.Y. Deng, H. Beppu, et al., Bone morphogenetic protein (BMP) type II receptor is required for BMP-mediated growth arrest and differentiation in pulmonary artery smooth muscle cells, J. Biol. Chem. 283 (2008) 3877–3888.
[62] M. Liberman, R.C. Johnson, D.E. Handy, et al., Bone morphogenetic protein-2 activates NADPH oxidase to increase endoplasmic reticulum stress and human coronary artery smooth muscle cell calcification, Biochem. Biophys. Res. Commun. 413 (2011) 436–441.
[63] N. Ferri, S. Marchiano, G. Tibolla, et al., PCSK9 knock-out mice are protected from neointimal formation in response to perivascular carotid collar placement, Atherosclerosis 253 (2016) 214–224.
[64] Y. Guo, Z. Tang, B. Yan, et al., PCSK9 (proprotein convertase subtilisin/kexin type 9) triggers vascular smooth muscle cell senescence and apoptosis: implication of its direct role in degenerative vascular disease, Arterioscler. Thromb. Vasc. Biol. (2021). ATVBAHA121316902.
[65] R. Nakano-Kurimoto, K. Ikeda, M. Uraoka, et al., Replicative senescence of vascular smooth muscle cells enhances the calcification through initiating the osteoblastic transition, Am. J. Physiol. Heart Circ. Physiol. 297 (2009) H1673–H1684.
[66] A.N. Kapustin, M.L. Chatrou, I. Drozdov, et al., Vascular smooth muscle cell calcification is mediated by regulated exosome secretion, Circ. Res. 116 (2015) 1312–1323.
[67] H.D. Jang, S.E. Lee, J. Yang, et al., Cyclase-associated protein 1 is a binding partner of proprotein convertase subtilisin/kexin type-9 and is required for the degradation of low-density lipoprotein receptors by proprotein convertase subtilisin/kexin type-9, Eur. Heart J. 41 (2020) 239–252.
[68] N. Sawada, Y. Taketani, N. Amizuka, et al., Caveolin-1 in extracellular matrix vesicles secreted from osteoblasts, Bone 41 (2007) 52–58.
[69] N.G. Seidah, S. Poirier, M. Denis, et al., Annexin A2 is a natural extrahepatic inhibitor of the PCSK9-induced LDL receptor degradation, PLoS One 7 (2012), e41865.
[70] A.N. Kapustin, J.D. Davies, J.L. Reynolds, et al., Calcium regulates key components of vascular smooth muscle cell-derived matrix vesicles to enhance mineralization, Circ. Res. 109 (2011) e1–12.
[71] C. Macchi, C.R. Sirtori, A. Corsini, et al., A new dawn for managing dyslipidemias: the era of rna-based therapies, Pharmacol. Res. 150 (2019) 104413.
[72] Y.M. Zhu, T.J. Anderson, K. Sikdar, et al., Association of proprotein convertase subtilisin/kexin type 9 (PCSK9) with cardiovascular risk in primary prevention, Arterioscler. Thromb. Vasc. Biol. 35 (2015) 2254–2259.
[73] P.M. Ridker, N. Rifai, G. Bradwin, et al., Plasma proprotein convertase subtilisin/kexin type 9 levels and the risk of first cardiovascular events, Eur. Heart J. 37 (2016) 554–560.
[74] B. Gencer, F. Montecucco, D. Nanchen, et al., Prognostic value of PCSK9 levels in patients with acute coronary syndromes, Eur. Heart J. 37 (2016) 546–553.
[75] K. Leander, A. Malarstig, F.M. Van't Hooft, et al., Circulating proprotein convertase subtilisin/kexin type 9 (PCSK9) predicts future risk of cardiovascular events independently of established risk factors, Circulation 133 (2016) 1230–1239.
[76] C. Werner, M.M. Hoffmann, K. Winkler, et al., Risk prediction with proprotein convertase subtilisin/kexin type 9 (PCSK9) in patients with stable coronary disease on statin treatment, Vasc. Pharmacol. 62 (2014) 94–102.
[77] C. Vlachopoulos, D. Terentes-Printzios, G. Georgiopoulos, et al., Prediction of cardiovascular events with levels of proprotein convertase subtilisin/kexin type 9: a systematic review and meta-analysis, Atherosclerosis 252 (2016) 50–60.
[78] J. Pott, V. Schlegel, A. Teren, et al., Genetic regulation of PCSK9 (proprotein convertase subtilisin/kexin type 9) plasma levels and its impact on atherosclerotic vascular disease phenotypes, Circ Genom Precis Med 11 (2018), e001992.
[79] M. Henein, G. Granasen, U. Wiklund, et al., High dose and long-term statin therapy accelerate coronary artery calcification, Int. J. Cardiol. 184 (2015) 581–586.
[80] I. Dykun, N. Lehmann, H. Kalsch, et al., Statin medication enhances progression of coronary artery calcification: the Heinz nixdorf recall study, J. Am. Coll. Cardiol. 68 (2016) 2123–2125.
[81] J.Z. Xian, M. Lu, F. Fong, et al., Statin effects on vascular calcification: microarchitectural changes in aortic calcium deposits in aged Hyperlipidemic mice, Arterioscler. Thromb. Vasc. Biol. (2021). ATVBAHA120315737.
[82] R.S. Rosenson, R.A. Hegele, S. Fazio, et al., The evolving future of PCSK9 inhibitors, J. Am. Coll. Cardiol. 72 (2018) 314–329.
[83] https://newsroom.heart.org/news/oral-pcsk9-inhibitor-found-to-be-safe-effective-to-lower-cholesterol-in-first-human-trial.
[84] https://esperion.gcs-web.com/node/12041/pdf.